Extrusion-shear of AZ31 Alloy Billets with Low Temperature and High Speed by Using Three-dimensional Finite Element Modeling and Experiments

Hu Hongjun, Zhai Zhiye, Wang Hao, Fan JunZhi*

College of Material Science and Engineering, Chongqing University of Technology, Chongqing, 400050, China

A new kind of compound extrusion technology including direct extrusion and shears for AZ31 magnesium billets can cause plastic large deformations and high strain rates. A series of compressive tests have been done to obtain the stress-strain curves of AZ31 magnesium alloy. Three-dimensional (3D) thermo-mechanical coupled finite element modeling of forming magnesium alloy AZ31billets into small rods at certain high ram speed and low temperature by extrusion-shears have been carried out. The simulation model has been established and meshed based on symmetrical characteristic. Computed parameters including material characteristics for workpiece and die and process conditions consisting of initial billet temperature, extrusion ratio, channel angle and ram speed have been list. The evolution of temperature during extrusion-shear process, there are hardly any temperature gradients within the workpiece, but temperature in severe plastic deformation zone increase rapidly. Strain evolutions for inner billet are larger than those of border positions. The flow velocity distribution is uniform basically which avoid the extrusion cracks to a certain degree. Experiments show that the rods with good surface smoothness can be obtained by low temperature and high speed extrusion-shear, and the alloy grains are effectively refined by dynamic recrystallization (DRX).

Keywords: *magnesium alloys, extrusion-shear, finite element modeling, dynamic recrystallization, temperature evolution, low extrusion temperature*

1. Introduction

Magnesium alloys is one of the lightest structural of engineering materials, but the crystal structures of magnesium alloys are hexagonal with poor cold workability, deformation mechanisms are only basal slip and twinning[1]. Bulk forming operations are normally carried on at elevated temperatures for additional slip systems would move, and become available to facilitate plastic deformation. Direct extrusion is one of the bulk-working processes. It is extensively used to produce wrought magnesium alloys[2]. Somjeet Biswas et al. have studied the evolution of the microstructure and crystallographic texture during torsion of a single phase magnesium alloy AM30, the results show that The observed microstructural features indicated the occurrence of continuous dynamic recovery and recrystallization[3]. Bulk nanostructure materials processed by methods of severe plastic deformation (SPD) such as equal channel angular extrusion (ECAE)[4]. Ramin Jahadi et al. has researched effect of ECAE process on the microstructure and mechanical properties of wrought AM30 magnesium alloy, The grain structure was refined from original size 20.4 μm to 3.9 μm through the four passes[5].

A new severe plastic deformation (SPD) method called Extrusion-Shears which included two consecutive processes initial forward extrusion and subsequent shears has been developed to fabricate fine grained AZ31 Mg alloys. K. Matsuyama et al. and Kiyoshi Matsubara et al. and many researchers used the EX-ECAP to prepare for the ultrafine magnesium[6,7], but the ECAP process was only used in the lab scale processing and preparation for nanocrystalline material, there exited an unbridgeable gap between the experimentation and applications of industry. The reference[8] demonstrates the feasibility of severe plastic deformation (SPD) techniques which combines conventional extrusion and equal channel angular pressing in a single process. It had yield strength of 310MPa and the ultimate tensile strength of 351MPa. The total elongation of 17.1% was about 2.5 times and the reduction in area of 42.5% was more than 10 times larger than the corresponding values in the as-received condition. Xibing Gong et al.[9] have researched the microstructure and mechanical properties of the twin-roll cast (TRC) Mg4.5Al1.0Zn alloy sheets produced by differential speed rolling (DSR) by optical microscopy, transmission electron microscope and electron backscattered diffraction. Orlov et al.[10] used an integrated process that combines conventional extrusion and equal channel angular pressing in a single processing step, and the processed material exhibited an excellent balance of strength and tensile ductility. Our research team engaged in the researches of the extrusion-shear process which included initial forward extrusion and shearing process subsequently as early as 2008[11]. Principal parameters for the extrusion-shear are the extrusion ratio, the initial temperature and speed of deformation, the frictional conditions and lubrication, etc.

*e-mail: 48516686@qq.com

Low temperature extrusion of magnesium alloy is done above the recrystallization temperature of the magnesium alloy. The advantages of low temperature extrusion can decrease oxidation of magnesium alloy, inprove strength and ductility. A new extrusion method is proposed, which may be called extrusion-shear which is shortened for extrusion-shear in this paper shown in Figure 1. Low temperature 370 °C extrusion-shear has been taken in the laboratory.

The evolutions of temperatures, strains, and stress and flow velocity of the billets during extrusion-shear are difficult to be described by tests and experiments. Numerical simulations can most likely research these evolution laws. Finite elements simulations can be used to obtain a better understanding of the refinements mechanisms for extrusion-shear process. There is a scarcity of information available in the open literature about 3D simulations for extrusion and shear. The present research was aimed to establish the evolution laws of temperatures and strain and flow velocities during the extrusion-shear of the AZ31 magnesium alloy billets into rods based on three-dimensional (3D) computer simulation.

2. Simulation Methods and Models

2.1. *Stress–Strain curves for AZ31 magnesium alloy*

The DEFORM™ -3D software package has been employed in the present research. Plasticity material has been used for the billet and a rigid material model for the dies. The elastic behaviors of the workpiece and tooling materials have been neglected in these material models. The flow stress–strain data of the AZ31 alloy were determined through hot compression tests by using Gleeble1500D machine. A set of flow stress/strain curves with temperature 300 °C are shown in Figure 1 as examples. To take the effect of deformation heat during hot compression at strain rates on the actual specimen temperature into account, a set of flow stress–strain curves include the experimental data over a temperature range of 250-450 °C and a strain rate range of 0.015-10s^{-1}. Plastic objects are modeled as rigid-plastic or rigid-viscoplastic material depending on characteristics of materials.

2.2. *Finite element models*

The geometric models formatted standard template library (shorten for STL) have imported to the finite element program DEFORM-3D v.6 software package to establish the finite element meshes. The original meshes of the billet and the cone-shaped die were divided as 20000 three-node triangular elements[12]. Increased element density can be done by object meshing of window especially deformation zone in the die. To save computing time and improve the mesh density, half of the workpiece and die and ram along the center of symmetry for longitudinal section have been modeled as Figure 2, the longitudinal section is defined as planar symmetry. Taking advantage of their symmetry and assuming the symmetry planes to be immobile and no material movement across these planes. Simulation and experimental parameters including dimensions of billet

and container are listed in Table 1, as well as the main process parameters used both in computer simulations and in extrusion-shear experiments. The simulation models consisted of 3 objects in the extrusion the billet, the die with an aperture diameter of 85 mm and a bearing length
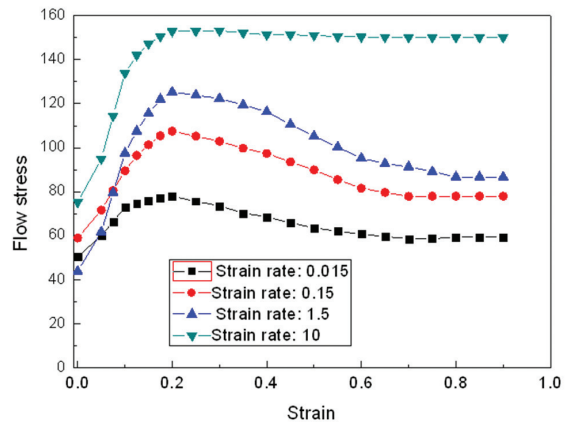

Figure 1. True stress/true strain curves of AZ31 obtained from compression tests with preheated temperature 300 °C.
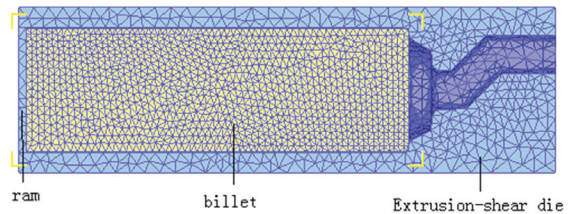

Figure 2. 3D Finite Element FEM Model selected for simulation with initial meshes.

Table 1. Simulation and experimental parameters for extrusion-shear.

Billet length /mm	250
Billet diameter /mm	80
Container insider diameter /mm	82
Container outside diameter (mm)	107
Die angle (°)	50
Channel angle (°)	135
Die bearing length (mm)	20
Extrusion ratio	10.24
Initial billet temperature (°C)	370
Initial tooling temperature (°C)	350
Ram speed (mm/s)	20
Friction factor of the container–billet interface	0.4
Friction factor between the billet and die.	0.4
Total number of elements for workpiece	20000
Mesh density type	Relative
Relative interference depth	0.7
Heat transfer coefficient between tooling and billet (N/ °C s mm²)	11
Heat transfer coefficient between tooling/billet and air(N/ °C s mm²)	0.02

2014; 17(4)

Extrusion-shear of AZ31 Alloy Billets with Low Temperature and High Speed
by Using Three-dimensional Finite Element Modeling and Experiments

989

of 20mm, and a rigid container. Both the container and the die regarded as rigid bodies, and the extrusion billet a rigid-plastic material have been considered in present analyses[13].

Wrought magnesium alloyAZ31 was used as the billet material in computer simulations and the properties are list in Table 2. The material for extrusion die, container and ram was the H13 hot-work tool steel. The simulation parameters used are listed in Table 1. The dimensions of billet and container are listed, as well as the main process parameters used in computer simulations. The ratio of die is 10.24

and channel angle is 135°. The initial billet temperature was selected to be 370 °C. In simulation, the temperature surrounding the container and die was set at 350 °C to avoid too much heat dissipation.

2.3. *Experiments*

Extrusion-shear experiments have been carried out to verify the results obtained from computer simulation in laboratory. In order to validate the results of finite element analysis, one set of tooling has been designed and manufactured to perform the actual extrusion processes, a

Table 2. Physical properties of the AZ31 workpiece.

Property	AZ31
Heat transfer coefficient between tooling and billet (N/ °C s mm²)	11
Heat transfer coefficient between tooling/billet and air(N/ °C s mm²)	0.02
Poisson's Ratio	0.35
Coefficient of linear expansion	26.8E-6
Density	1780 kg/m³
Poison's ratio	0.35
Young's modulus	45000Mpa
Emissivity	0.12

extrusion-shear die with die angle 50° and channel angle 135° has been designed and manufactured with a uniform bearing length of 20 mm shown in Figure 3. Extrusion-shear die consists of direct extrusion and two continuous channels which have an equal round cross-section. The design of extrusion-shear has been not well known or understood by the public. It is interpreted as that the technology or the mechanism regarding the extrusion-shear die design and the plastic deformation has not been fully developed yet. In order to understand the behaviors of the plastic deformation for extrusion-shear, dies have been designed and manufactured.

Before the extrusion the billets have been machined to a diameter of 80 mm. The extrusion-shear experiments have been carried out by employing a 500 ton press with a resistance heated container and a heater. The die material, die dimensions, billet dimensions and extrusion conditions were all the same as those used in numerical simulation as described above. The billet was heated in an external furnace up to 370 °C and transported into the container at a preset temperature of 350 °C to avoid too much heat dissipation and then extrusion started immediately. The ram speed was 20mm/s during experimental verification.

The chemical composition of the as-received AZ31 billet used in this study (in mass percent) is Mg3.02% Al1.01% Zn0.30%Mn. All the observation samples have been taken from the center of rod. Microstructures in the as-received and extrusion-shear extruded materials are examined following standard metallographic procedures. The polished surface is etched using either a solution of 1 vol%HNO_3, 24 vol%$C_2H_6O_2$, and 75 vol% H_2O, or of 10 milliliter acetic acid, 4.2 g picric acid, 10 milliliter H_2O, or 70 milliliter ethanol. Microstructure observations have been carried out using PME OLYMPUS TOKYO-type optical microscope (OM).
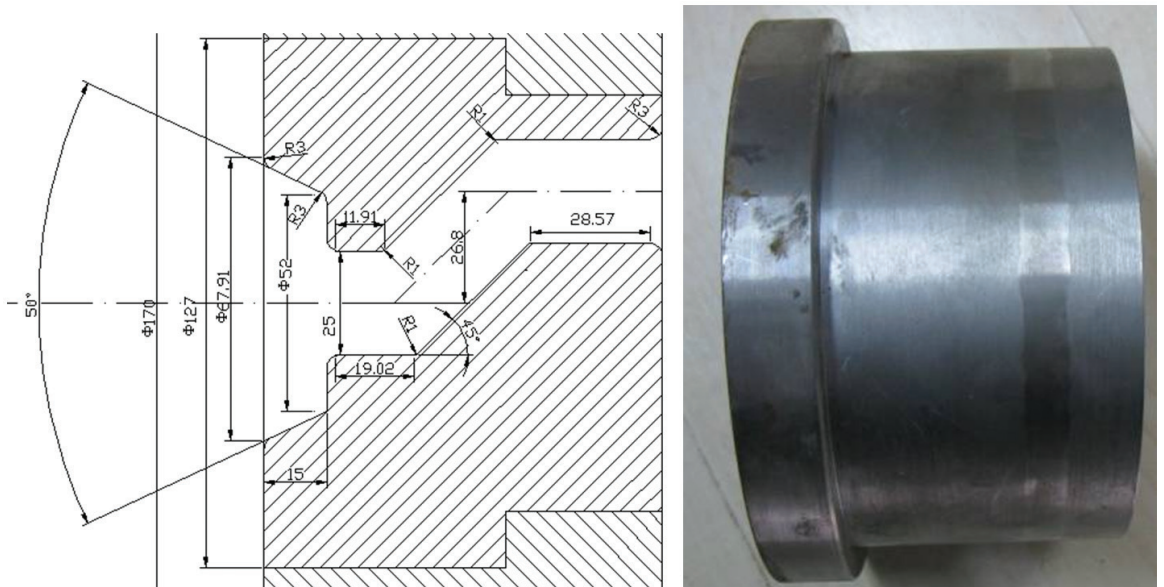

Figure 3. (a) Schematic diagram of an extrusion-shear die, (b) Structure of extrusion-shear die.

3. Results and Discussion

Extrusion-shear was simulated from the start of extrusion until the extrusion was steady state. In order to analyze the stress, effective strain and temperature distribution of specimen during extrusion, the temperatures

Figure 4. Variations of the maximum and minimum temperatures during extrusion-shear at a ram speed of 20 mm/s.

and strains and flow velocities and stress distributions of the billet as well as the deformation behavior of the billet have been predicted during extrusion by using Deform software.

3.1. *Temperature evolution during extrusion-shear*

The evolution of temperature during extrusion-shear process can be influenced by deformational and frictional heat. The final average material temperature T_m at a time t is as Equations 1[14].

$$T_m = T_d + T_f + T \tag{1}$$

Where T_d is temperature for frictionless deformation process, T_f temperature increase due to friction, T initial preheated temperature of billet. In this paper the frictional factors is the constant and equal to 0.4, the temperature rise depends on the die structures including the contact area between the billet and die, the size of the deformation zone and extrusion ratio and process parameters.

The variations of the maximum temperature and minimum temperature in the workpiece during extrusion-shear process cycle are shown in Figure 4. The figure shows that variation of the maximum temperature rise. From the curve of maximum temperature curve, the temperature is near 370 °C at the beginning of the process, the maximum
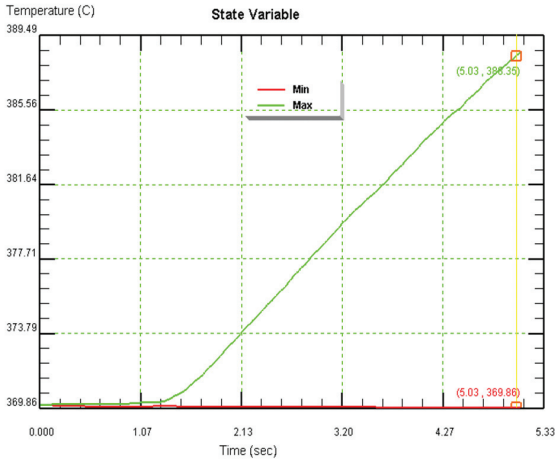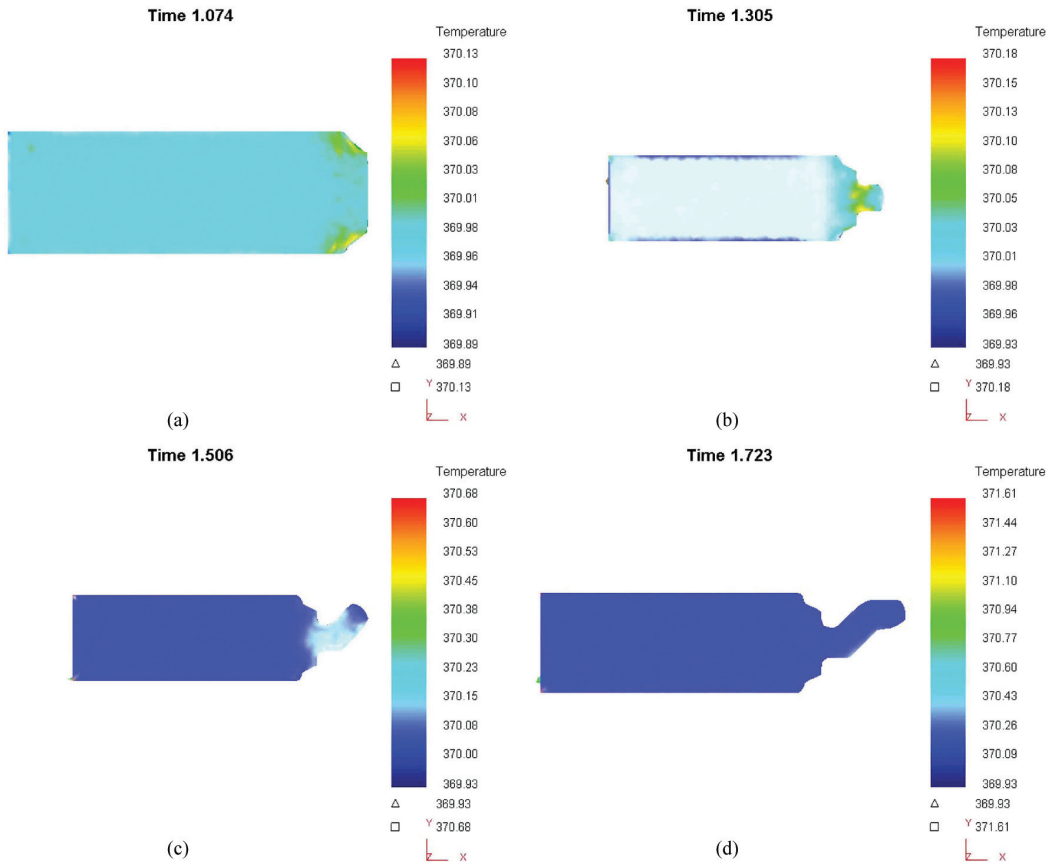

Figure 5. Evolution of temperature fields during extrusion-shear with ram speed 20 mm/s and low temperature. (a) 1.047s, (b) 1.305s, (c) 1.506s, (d) 1.723s.

2014; 17(4)

Extrusion-shear of AZ31 Alloy Billets with Low Temperature and High Speed
by Using Three-dimensional Finite Element Modeling and Experiments

991

workpiece temperature is linear increase steeply after extrusion time 1.272 s for more heat is generated and less heat lost. Since the temperature rise depends on the heat generated within the deformation zone. And heat generation in billets depends on the plastic deformation power and frictional power.

Figures 5a and b shows the temperature evolution during direct extrusion period of extrusion-shear process with ram speed of 20mm/s before two continue shears. It is clear that the temperature in the most part of the billet decreases during direct extrusion, the maximum temperature near the die bearing rises for plastic deformation around the die workland can generate a large amount of heat to raise the temperature of billet. The main feature of the temperature evolution is that the temperature in the rear part away from the die entrance decreases gradually. At the edge of the billet in contact with both the container the temperature is lowest for more heat has been lost.

Figures 5c and d show the temperature distributions during two shearing period of extrusion-shear process. Compared with the temperature evolution in the direct extrusion phase, the temperatures of the billet in the zone in front of the die exit altered little. The simulation results clearly show that there are hardly any temperature gradients within the workpiece, the billet and tooling during the extrusion-shear process.

3.2. Strain and stress evolutions for extrusion-shear

The principle of extrusion-shear process is to introduce compressive and accumulated shear strains into the samples. Strain is defined as the sum of a large series of arbitrarily small strain increments. A detailed description of strain is available in any standard text on mechanics of materials, metal forming analysis, or plasticity. The distributions of strains in Figure 6 show that the strain distribution is relatively steady during extrusion-shear process. In the severe deformation zone in front of the die exit, strains remain higher than 0.4. The strains are even higher than 3 in the billet near the die exit. And the effective strains range is between 0.1 and 2.96. It is clear that maximum strains in the workpiece lie in the plastic deformation zone.

The characters of extrusion-shear process are that the sample is subjected to two shearing deformation. The accumulative strains of extrusion-shear can be expressed as Equations 2 which include two parts which are accumulative strain of direct extrusion and two continuous ECAE steps, which combine expression of ECAE strain and the accumulation strain of direct extrusion[15].

$$\varepsilon = \ln\lambda + 2 * \left[\frac{2\cot\left(\frac{\phi}{2} + \frac{\psi}{2}\right) + \psi\csc\left(\frac{\phi}{2} + \frac{\psi}{2}\right)}{\sqrt{3}} \right] \quad (2)$$
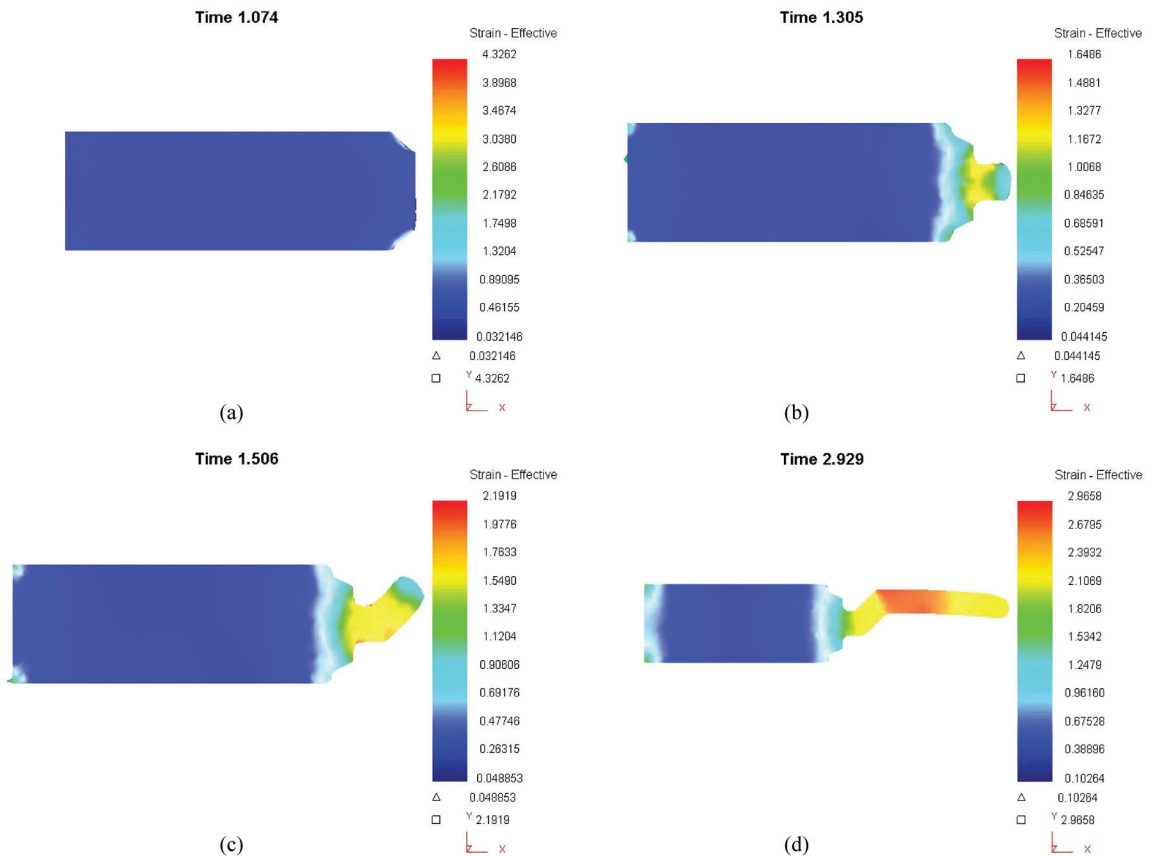

Figure 6. Strains evolution during extrusion-shear with ram speed 20 mm/s.1.047s, (b) 1.305s, (c) 1.506s, (d) 1.723s.

Where ε is the accumulative strain, λ the extrusion ratio, ϕ the inner channel angle, Ψ the outer channel angle.

Particle tracking method is performed to analyze strain and stress evolution for certain points during extrusion-shear process. To illustrate the strain changing with ram displacement clearly, the strain and stress at selected points "p1" and "p2" and "p3"in the severe deformation zone of Figure 7 have been tracked. The evolution of effective strains has been shown at these points in Figure 8. It is clear that effective strains of these points increase rapidly from 0 to 1.02-1.5, during direct extrusion till extrusion time 1.305 s. During subsequent continuous shear period, effective strains at points " p_2" increase slowly to a value of 2.01 and then begin to increase slowly. But the strains increase to 1.41, and then decrease to about 0.8 for the p_1 and p_3. It is obvious that strain evolutions for inner billet is larger than those of other positions. When the deformation reaches steady the strains increase slowly. When the AZ31 magnesium alloy flows into the severe deformation zone, severe deformation occurs and a large amount of plastic deformation heat is generated. During direct extrusion, effective stresses at these points are about 88-159MPa at the end of shear period, as shown in Figure 9. During continuous shearing period the stress for p_2 decreases firstly, and then remains steady. And stresses of p_1 and p_3 are fluctuation and the lowest value is about 64 MPa.

3.3. *Flow velocity during extrusion-shear*

Figure 10 shows the metal flow velocities during extrusion-shear process and each zone that extrusion-shear process is classified into (a) compression zone, (b) direction extrusion zone, (c) first shearing zone and (d) second shearing zone. Firstly, initial billet is compressed in direction extrusion zone and the final rod diameter obtained, Secondly material is sheared during first shearing zone, thirdly the materials are endured the second shearing and come out of die during second shearing zone. It is obvious that a small dead metal zone exists near compression zone of die in Figure 10a, and there is an obvious metal flow interface, where metal moves perpendicular to the die wall. In Figure 10b the direct extrusion stage is over. The metal flow velocities improve rapidly from 17mm/s to 130mm/s. In the Figures 10c and d the metal near the container flows towards the die homogeneously. The metal flow direction is not along the extrusion direction at exit of die, but there exits an angle with the direction of extrusion, which would cause the bending rods.

3.4. *Experimental results and analysis*

An AZ31B rod extruded at temperature 370 °C with channel angle 135° is shown in Figure 11a.

It is founded that products have been found with better surface finish, but there exits bending defects. There were some inherent drawbacks for microstructures of extrusion process due to uneven metal flow during extrusion-shear which causes the properties from surface to the center uneven. But the use of extrusion-shear process, the average grain size can be changed from 250 μm (as cast state) to 10 μm, the microstructures are not only clearly refined but also relatively uniform. This was because the extrusion-shear
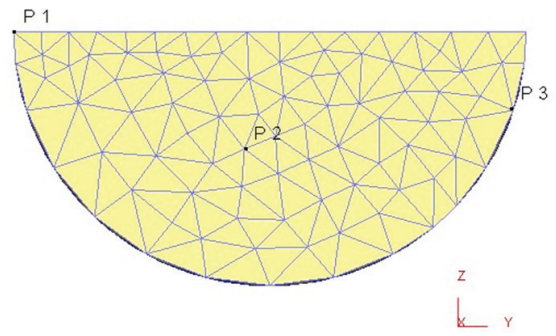

Figure 7. Selected points in the cross section of billet for the analysis of effective strain and effective stress evolution.
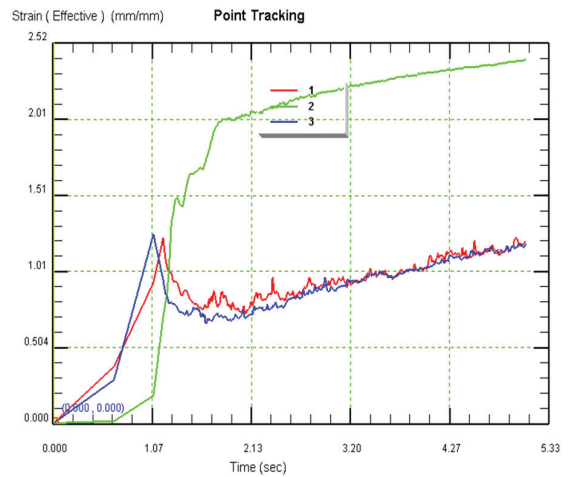
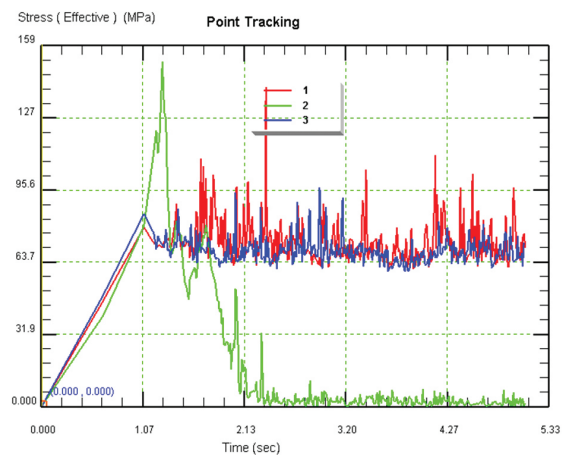

Figure 8. Evolution of effective strains for point p_1, p_2 and p_3.

Figure 9. Evolution of effective stresses for point p_1, p_2 and p_3.

process included two simple shear extrusion processes more than an ordinary extrusion. So that the deformation degree of central part of rods increased, the part recrystallization occurred. Therefore, the microstructures became finer and more homogeneous.
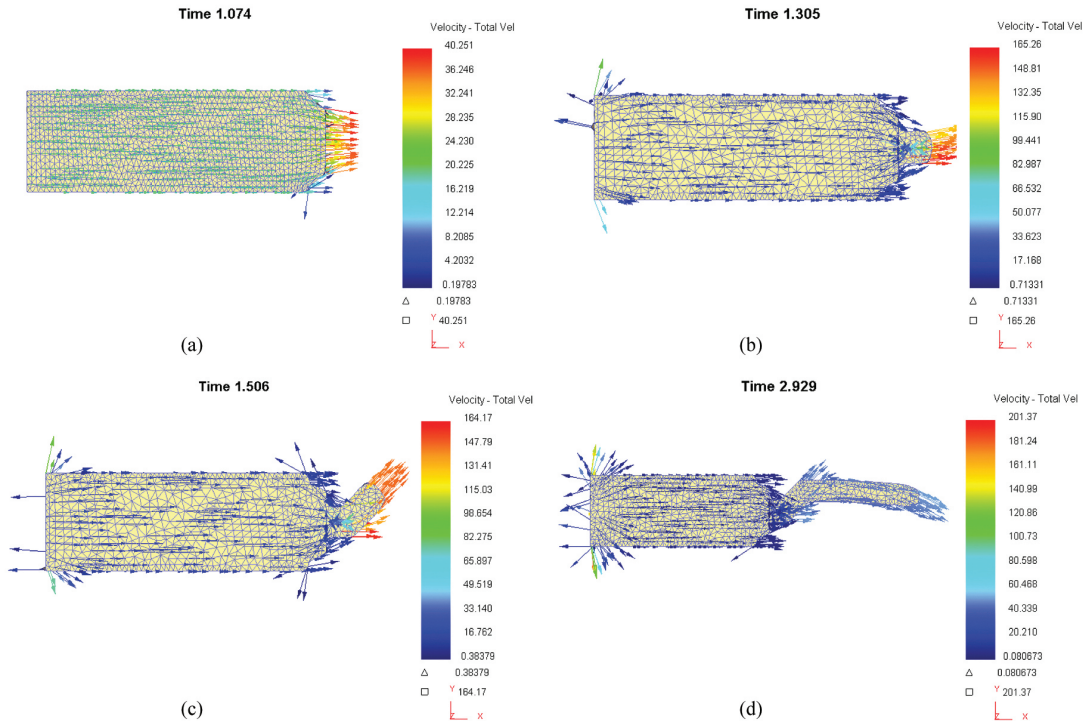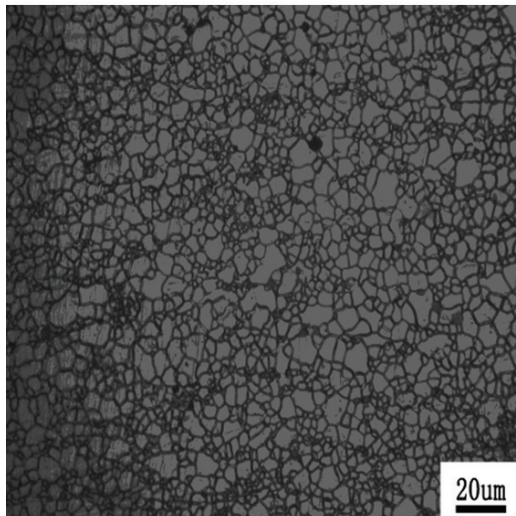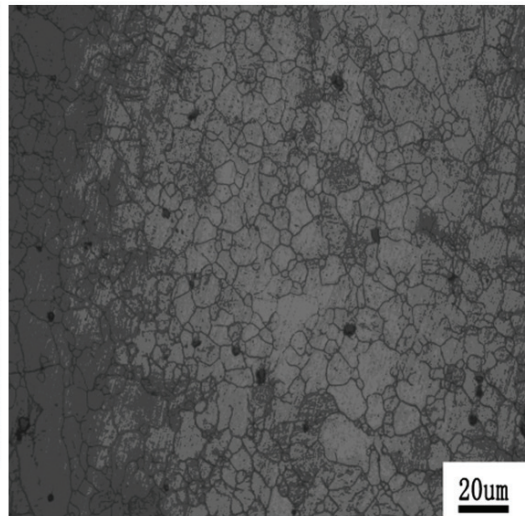
2014; 17(4)

Extrusion-shear of AZ31 Alloy Billets with Low Temperature and High Speed
by Using Three-dimensional Finite Element Modeling and Experiments

993

Figure 10. The flow velocity fields during the extrusion, (a) 1.047s, (b) 1.305, (c) 1.506s and (d) 2.929s.

Figure 11. Extrusion products in laboratory rod extruded by bottom die with channel angle 135° (a), Microstructures of AZ31 magnesium alloy in longitudinal section (b) and cross section (c).

AZ31 Mg alloy have been prepared through ES die with channel angles 135°. From the metallographic Figures 11b and c. After extrusion-shear process the alloy grains are effectively refined by dynamic recrystallization (DRX) and continuous shears. It could be found that some tiny subgrains appear around original coarse grains. The dynamic recrystallization fraction is a function of strain, strain rate, temperature. The Avrami equation is used to describe the relation between the dynamically recrystallized fraction X and the effective strain[16,17].

$$X_{drex} = 1 - \exp\left[-\beta_d \left(\frac{\varepsilon - a_{10}\varepsilon_p}{\varepsilon_{0.5}}\right)^{k_d}\right] \quad\quad (3)$$

- X_{drex} is dynamically recrystallized fraction, β_d k_d material data, ε strain, ε_p Peak strain,

- $\varepsilon_{0.5}$ strain for 50% recrystallization.

From the Equation 3, the dynamically recrystallized fraction X_{drex} increases with the effective strain increasing. It can be concluded that the dynamically recrystallized fraction caused by extrusion-shear die with angle 135°. The principle of extrusion-shear process is to introduce compressive and accumulated shear strain into the rod for magnesium alloy. The characters of extrusion-shear process are that the sample is subjected to two shear deformation[5,8]. The accumulative strains of extrusion-shear include accumulative strain of direct extrusion and two continuous ECAE steps. It can be found that the accumulative strain increase with the extrusion advancing, so the grains will be refined consequently.

4. Conclusions

The finite element models including the mathematical models and geometric models and solution conditions have been applied to calculate the temperature and strain and stress and flow velocity fields of billet during extrusion-shear process. Initial billet temperature, friction factor and extrusion speed etc. are the main parameters that affect the evolution of billet temperature and strain. The temperature in the most part of the billet decreases during direct extrusion, the maximum temperature near the die bearing rises for plastic deformation around the die workland can generate a large amount of heat to raise the temperature of billet. There are hardly any temperature gradients within the workpiece, the billet and tooling during the shear period, and the maximum temperature increases significantly. Maximum strains in the entire workpiece are seen in the plastic deformation zone during extrusion-shear process. The strain and stress of the metal in the billets are various during extrusion-shear process. Extruded AZ31 sample showed a fine-grained microstructure and some grain size gradient throughout cross section. The theoretical analysis shows that the extrusion-shear would cause serve plastic deformation and improve the dynamic recrystallization and shear fracture of grains during extrusion.

Acknowledgements

References

1. Song HR, Kim YS and Nam WJ. Mechanical Properties of Ultrafine Grained 5052 Al Alloy Produced by Accumulative Roll-Bonding and Cryogenic Rolling. *Metals and Materials International*. 2006; 12(1):7-13. http://dx.doi.org/10.1007/BF03027516

2. Lee SC, Ha SY, Kim KT, Hwang SM, Huh LM and Chung HS. Finite element analysis for deformation behavior of an aluminum alloy composite containing SiC particles and porosities during ECAP. *Materials Science and Engineering A*. 2004; 371(1-2):306-312. http://dx.doi.org/10.1016/j.msea.2003.12.029

3. Biswas S, Beausir B, Toth LS and Suwas S. Evolution of texture and microstructure during hot torsion of a magnesium alloy. *Acta Materialia*. 2013; 61(14):5263-5277. http://dx.doi.org/10.1016/j.actamat.2013.05.018

4. Chen YJ, Wang QD, Lin JB, Zhang LJ and Zhai CQ, Microstructure and mechanical properties of AZ31 Mg alloy processed by high ratio extrusion [J]. *Transactions of Nonferrous Metals Society of China*. 2006; 16(S3):S1875-S1878.

5. Jahadi R, Sedighi M and Jahed H. ECAP effect on the microstructure and mechanical properties of AM30 magnesium alloy. *Materials Science & Engineering A*. 2014; 593:178-184. http://dx.doi.org/10.1016/j.msea.2013.11.042

6. Matsuyama K, Miyahara Y, Horita Z and Langdon TG. Developing superplasticity in a magnesium alloy through a combination of extrusion and ECAP. *Acta Materialia*. 2003; 51(11):3073-3084. http://dx.doi.org/10.1016/S1359-6454(03)00118-6

7. Matsubara K, Miyahara Y, Horita Z and Langdon TG. Achieving Enhanced Ductility in a Dilute Magnesium Alloy through Severe Plastic Deformation. *Metallurgical and Materials Transactions A*. 2004; 35(6):1734-1744.

8. Yang Q, Jiang B, Zhou G, Dai J and Pan F. Influence of an asymmetric shear deformation on microstructure evolution and mechanical behavior of AZ31 magnesium alloy sheet. *Materials Science Engineering A*. 2014; 590(1):440-447. http://dx.doi.org/10.1016/j.msea.2013.10.045

9. Gong X, Li H, Kang SB, Cho JH and Li S. Microstructure and Mechanical Properties of Twin-roll Cast Mg-4.5Al-1.0Zn Alloy Sheets Processed by Differential Speed Rolling. *Materials and Design*. 2010; 31(3):1581-1587. http://dx.doi.org/10.1016/j.matdes.2009.09.021

10. Orlov D, Raab G, Lamark TT, Popov M and Estrin Y. Improvement of mechanical properties of magnesium alloy ZK60 by integrated extrusion and equal channel angular pressing. *Acta Materialia*. 2011; 59(1):375-385. http://dx.doi.org/10.1016/j.actamat.2010.09.043

2014; 17(4)

Extrusion-shear of AZ31 Alloy Billets with Low Temperature and High Speed
by Using Three-dimensional Finite Element Modeling and Experiments

995

11. Hu H, Zhang D and Zhang J. Microstructures in an AZ31 magnesium alloy rod fabricated by a new SPD process based on Physical Simulator. *Transactions of Nonferrous Metals Society of China*. 2010; 20(3):478-483.

12. Liu Y, Tang Z, Zhou K and Li Z. Equal channel angular pressing process of pure aluminum(II) -Simulation of deformation behavior. *Chinese Journal of Nonferrous Metals*. 2003; 13(2):294-299.

13. Hu H, Zhang D, Yang M and Deng M. Grain refinement in AZ31 Magnesium alloy rod fabricated by an ES SPD process. *Transactions of Nonferrous Metals Society of China*. 2011; 21(2):243-249. http://dx.doi.org/10.1016/S1003-6326(11)60705-X

14. Watanabe H, Tsutsui H, Mukai T, Ishikawa K, Okanda Y, Kohzu M et al. Grain size control of commercial wrought Mg-Al-Zn alloys utilizing dynamicrecrystallization. *Materials Transactions*. 2001; 42(7):1200-1205. http://dx.doi.org/10.2320/matertrans.42.1200

15. Hu H, Zhang D, Pan F and Yang M. Analysis of the Cracks Formation on Surface of Extruded Magnesium Rod Based on Numerical Modeling and Experimental Verification. *Acta Metallurgica Sinica*. 2009; 22(5):353-364. http://dx.doi.org/10.1016/S1006-7191(08)60109-X

16. Scientific Forming Technologies Corporation. *User's Manual for DEFORMTM -3D Version 6.1*. 2007.

17. Liu J, Wanga Q, Zhou H and Guo W. Microstructure and mechanical properties of NZ30K magnesium alloy processed by repetitive upsetting. *Journal of Alloys and Compounds*. 2014; 589(3):372-377. http://dx.doi.org/10.1016/j.jallcom.2013.12.008